

Use of cortical volume to predict response to temporary CSF drainage in patients with idiopathic normal pressure hydrocephalus

Stefan Lang, MD, PhD,¹ Dennis Dimond, PhD,³ Albert M. Isaacs, MD, PhD,²
Jarred Dronyk, MA, MHS,³ Artur Vetkas, MD, PhD,¹ Christopher R. Conner, MD, PhD,¹
Jurgen Germann, PhD,¹ Alfonso Fasano, MD, PhD,^{4–6} Suneil Kalia, MD, PhD,^{1,6}
Andres Lozano, MD, PhD,^{1,6} and Mark G. Hamilton, MDCM³

¹Department of Neurosurgery, University of Toronto, Ontario, Canada; ²Department of Neurosurgery, Vanderbilt University, Nashville, Tennessee; ³Department of Clinical Neurosciences, Division of Neurosurgery, University of Calgary, Cumming School of Medicine, Calgary, Alberta, Canada; ⁴Edmond J. Safra Program in Parkinson's Disease, Morton and Gloria Shulman Movement Disorders Clinic, Toronto Western Hospital, UHN, Toronto, Ontario, Canada; ⁵Division of Neurology, University of Toronto, Ontario, Canada; and ⁶Krembil Brain Institute, Toronto, Ontario, Canada

OBJECTIVE Temporary drainage of CSF with lumbar puncture or lumbar drainage has a high predictive value for identifying patients with suspected idiopathic normal pressure hydrocephalus (iNPH) who may benefit from ventriculoperitoneal shunt insertion. However, it is unclear what differentiates responders from nonresponders. The authors hypothesized that nonresponders to temporary CSF drainage would have patterns of reduced regional gray matter volume (GMV) as compared with those of responders. The objective of the current investigation was to compare regional GMV between temporary CSF drainage responders and nonresponders. Machine learning using extracted GMV was then used to predict outcomes.

METHODS This retrospective cohort study included 132 patients with iNPH who underwent temporary CSF drainage and structural MRI. Demographic and clinical variables were examined between groups. Voxel-based morphometry was used to calculate GMV across the brain. Group differences in regional GMV were assessed and correlated with change in results on the Montreal Cognitive Assessment (MoCA) and gait velocity. A support vector machine (SVM) model that used extracted GMV values and was validated with leave-one-out cross-validation was used to predict clinical outcome.

RESULTS There were 87 responders and 45 nonresponders. There were no group differences in terms of age, sex, baseline MoCA score, Evans index, presence of disproportionately enlarged subarachnoid space hydrocephalus, baseline total CSF volume, or baseline white matter T2-weighted hyperintensity volume ($p > 0.05$). Nonresponders demonstrated decreased GMV in the right supplementary motor area (SMA) and right posterior parietal cortex as compared with responders ($p < 0.001$, $p < 0.05$ with false discovery rate cluster correction). GMV in the posterior parietal cortex was associated with change in MoCA ($r^2 = 0.075$, $p < 0.05$) and gait velocity ($r^2 = 0.076$, $p < 0.05$). Response status was classified by the SVM with 75.8% accuracy.

CONCLUSIONS Decreased GMV in the SMA and posterior parietal cortex may help identify patients with iNPH who are unlikely to benefit from temporary CSF drainage. These patients may have limited capacity for recovery due to atrophy in these regions that are known to be important for motor and cognitive integration. This study represents an important step toward improving patient selection and predicting clinical outcomes in the treatment of iNPH.

<https://thejns.org/doi/abs/10.3171/2023.3.JNS222787>

KEYWORDS cerebrospinal fluid; lumbar drain; normal pressure hydrocephalus; tap test; machine learning

ABBREVIATIONS CAT12 = Computational Anatomy Toolbox; DESH = disproportionately enlarged subarachnoid space hydrocephalus; ELD = external lumbar drainage; FDR = false discovery rate; FN = false negative; FP = false positive; GMV = gray matter volume; iNPH = idiopathic normal pressure hydrocephalus; LOOCV = leave-one-out cross-validation; LP = lumbar puncture; MNI = Montreal Neurological Institute; MoCA = Montreal Cognitive Assessment; NPV = negative predictive value; PPV = positive predictive value; SMA = supplementary motor area; SVM = support vector machine; TN = true negative; TP = true positive; VBM = voxel-based morphometry; VPS = ventriculoperitoneal shunt.

SUBMITTED January 9, 2023. **ACCEPTED** March 23, 2023.

INCLUDE WHEN CITING Published online May 5, 2023; DOI: 10.3171/2023.3.JNS222787.

IDIOPATHIC normal pressure hydrocephalus (iNPH) is an age-related syndrome of gait dysfunction, cognitive impairment, and urinary incontinence associated with an enlarged ventricular system in the absence of elevated intracranial pressure.¹ iNPH is a common disease, affecting 1.3% of those aged 65 years and increasing to affect 5.9% of the population by the age of 85 years.^{2,3} The pathophysiology has remained elusive, although several theories have been proposed.² These include impairments of CSF dynamics,^{4,5} alterations in regional brain perfusion,^{6,7} impaired glymphatic system function,^{8,9} white matter injury,^{10,11} gray matter atrophy,¹² and alterations in functional brain networks.^{13,14}

Despite the uncertainty regarding the pathophysiological mechanisms, clinicians have long been aware that drainage of CSF can result in clinical improvement, with as many as 80% of properly selected patients responding to ventriculoperitoneal shunt (VPS) placement.^{15,16} Proper selection of patients requires excluding those whose symptoms are not attributable to ventriculomegaly. After exclusion of other diagnoses, patients are considered to have suspected iNPH. However, only a subset of these patients will have a positive response to CSF drainage. To avoid the unnecessary risk associated with permanent VPS insertion, patients with suspected iNPH typically undergo prognostic testing with temporary CSF drainage via a large-volume lumbar puncture (LP) or external lumbar drainage (ELD). Those who respond positively undergo VPS implantation, whereas the subgroup that fails to respond is left with minimal treatment options.

It is currently unclear what differentiates responders from nonresponders to temporary CSF drainage. Both groups have a similar clinical phenotype with enlarged ventricles (Evans index ≥ 0.3), yet only 30.7%–77.8% of patients have a positive response to prognostic tests and undergo shunt surgery.¹⁶ Determining the features that predict a poor response could further our understanding of the pathophysiology of iNPH and the mechanism of treatment success. Furthermore, this could help clinicians be more selective about implementing prognostic tests, as there are small risks but not insignificant healthcare system costs associated with tap tests and lumbar drain insertion. One specific hypothesis is that nonresponders to CSF drainage have decreased regional gray matter volume (GMV) that may limit the positive response to CSF drainage.

The aim of the current study was to assess the relationship between GMV and response to temporary CSF drainage in a large group of suspected iNPH patients who were evaluated at a specialized hydrocephalus center. We hypothesized that nonresponders to CSF drainage would have decreased regional GMV identified with voxel-based morphometry (VBM). Secondary analyses were aimed at relating extracted GMV differences to clinical outcomes and using GMV in a machine learning model to predict clinical response.

Methods

Subjects

In this retrospective cohort study, we identified 171 patients who were referred to the University of Calgary Adult

Hydrocephalus Clinic with suspected iNPH between 2018 and 2021 and had undergone structural MRI acquisition and prognostic testing with temporary CSF drainage during their clinical evaluation. Subjects provided informed consent, and the study was approved by the University of Calgary Research Ethics Board. Thirty-nine patients were excluded from the analysis secondary to MRI acquisition details (see the *MRI Acquisition* and *MRI Analysis* sections). This resulted in a final cohort of 132 patients with suspected iNPH and good-quality MRI scans who were included in the analysis.

Clinical and Temporary CSF Drainage Assessments

Suspected iNPH was defined to include patients with typical symptoms (cognitive decline, urinary incontinence, and gait and balance difficulties) and ventriculomegaly (Evans index ≥ 0.3), and those with other possible confounding diagnoses were excluded.¹⁷ Each patient underwent detailed clinical assessments in a specialized hydrocephalus clinic before and after temporary CSF drainage. The clinical assessment included measures of cognition (Montreal Cognitive Assessment [MoCA]) and 10-m gait velocity. These patients underwent temporary CSF drainage with ELD (n = 116) or large-volume LP (n = 16).¹⁶ All negative LP patients subsequently underwent ELD. The ELD trial consisted of a 3-day inpatient hospital admission with CSF drainage of 10 ml/hr. The drain was removed after the 3rd day, and patients were examined shortly after. LP consisted of a one-time removal of 50 ml, with a repeat examination 4–6 hours after.

Due to language constraints or inability to perform tasks, some patients did not undergo preprocedural and postprocedural MoCA and gait velocity testing, leaving 100 with complete MoCA data and 118 with complete gait velocity data. A gait velocity score of 0 m/sec was assigned if patients could not complete the 10-m walk test due to significant impairment. All 132 patients were classified as responders or nonresponders regardless of the ability to complete MoCA and gait velocity testing. Responders were identified by the attending hydrocephalus physician (M.G.H.) after taking into consideration changes in gait velocity or MoCA scores. A clinically significant change in gait velocity was defined as an improvement $\geq 20\%$ between the preprocedural and postprocedural CSF drainage assessments. In addition to the evaluation of quantitative measures, the decision to offer treatment with a VPS also included elements based on clinical expertise. All responders were subsequently offered VPS insertion.

MRI Acquisition

T1-weighted anatomical MR images were collected on a total of four 1.5-T and one 3.0-T clinical MRI scanners, each with an 8-channel head coil at hospitals across Calgary. Six distinct scanning sequences were used. Scanner details, including acquisition parameters, can be found in Supplementary Table 1. To correct for the nonbiological variance introduced by differences in the MRI scanners, we utilized the ComBat harmonization procedure.¹⁸ ComBat is a batch-effect correction tool commonly used in genomics¹⁹ and more recently for removal of scanner effects

in multisite neuroimaging studies.^{20–22} It has been shown to successfully remove unwanted sources of scan variability from multisite studies, while simultaneously retaining variability attributed to effects of interest and increasing the power of subsequent statistical analysis.^{18,23} Patients ($n = 39$) were excluded from the study if they had incomplete MRI data (e.g., prematurely terminated scan, part of the brain was outside of the field of view), gadolinium-enhanced images, acquisition parameters that were inconsistent with the majority of the subjects whose data were collected on the same scanner, or if the images had failed or had unsatisfactory segmentation due to poor quality.

MRI Analysis

We assessed GMV with VBM²⁴ in SPM12 by using the Computational Anatomy Toolbox (CAT12)²⁵ (<http://141.35.69.218/cat/>) and standard preprocessing procedures, including a formal assessment of image quality (Supplementary Fig. 1).²⁶ Patients with an image quality rating less than the cutoff of 70,^{25,26} indicating unsatisfactory quality for segmentation, were excluded. T1-weighted images were segmented into gray matter, white matter, and CSF. Segmentations were coregistered to a study-specific anatomical template created using DARTEL²⁷ (Diffeomorphic Anatomical Registration Using Exponentiated Lie Algebra) and subsequently normalized to Montreal Neurological Institute (MNI) space. Scans were visually assessed at each stage of preprocessing to ensure quality and were excluded from further analysis if contaminated by gross artifacts or segmentation failure. Normalized images were modulated to preserve the initial amounts of gray and white matter present in each voxel prior to their spatial warping. Smoothing (8-mm full width at half maximum gaussian kernel) was performed to mitigate between-subject differences in spatial normalization and to satisfy the assumptions of parametric statistical testing. Along with GMV, we extracted the relative volume of CSF and relative volume of T2-weighted white matter hyperintensities by using the segmentation procedure. This latter procedure was done using the T1-weighted images, as implemented in CAT12.²⁸ For each patient, standard clinical MRI data were extracted, including the following: Evans index (ratio between the maximum diameter of the frontal horns and the maximum inner skull diameter in the slice above the foramen of Monro), callosal angle (the angle between the lateral ventricles on the coronal slice at the level of the posterior commissure), and the presence or absence of disproportionately enlarged subarachnoid space hydrocephalus (DESH) (which was considered present when there were signs of sylvian fissure dilation in conjunction with obliterated sulci at the high convexity).

Statistical Analysis

Statistical analysis of demographic data, relative volume of CSF, relative volume of total GMV, and relative volume of white matter hyperintensities was performed in MATLAB version R2018B (MathWorks). The Kolmogorov-Smirnov test was used to assess for normality. Demographic variables were compared between groups with the two-sample t-test, chi-square test (for categorical

data), or Mann-Whitney U-tests (for nonnormally distributed data).

Following correction for scanner effects with ComBat harmonization, GMV was compared between groups (responder vs nonresponders) while adjusting for total intracranial volume and type of procedure performed (ELD vs LP). This was performed on a voxel-wide basis with the ANCOVA test and implemented in SPM12. Cluster thresholding was utilized with an initial voxel threshold of $p < 0.001$ and a cluster threshold of $p < 0.05$, with false discovery rate (FDR) correction for multiple comparisons. To improve confidence, we repeated this whole-brain analysis 10 times with random permutation (sampling without replacement) of responder/nonresponder subject labels. We also repeated the analysis using only the group of patients who underwent ELD, while excluding those who underwent LP. For the groups of patients with complete preprocedural and postprocedural MoCA ($n = 100$) and gait velocity ($n = 118$) data, we assessed the relationships of the change in MoCA score and change in gait velocity with the average GMV values extracted from the clusters; this analysis demonstrated a significant difference between groups. This was performed with linear regression, with significance set at $p < 0.05$ (uncorrected).

Machine Learning Analysis

Machine learning analysis was used to derive a predictive model of clinical outcome. We used demographic data and extracted GMV features to train a support vector machine (SVM) to classify response status. The model was validated with leave-one-out cross-validation (LOOCV). This was performed with the MATLAB functions `fitcsvm` and `crossval` and employed a radial basis function kernel. Predictors included the extracted GMV values from the responder versus nonresponder analysis, along with age and callosal angle. LOOCV trains the model with data from $n - 1$ samples (131) and subsequently classifies the left-out subject. This is repeated n times (132), allowing for classification of each subject based on training from every other subject. Following this, a confusion matrix was created to assess the true-positive (TP), false-positive (FP), true-negative (TN), and false-negative (FN) rates. The accuracy ($(TP+FP)/n$), precision/positive predictive value (PPV) ($TP/(TP+FP)$), negative predictive value (NPV) ($TN/(TN+FN)$), recall/sensitivity ($TP/(TP+FN)$), specificity ($TN/(FP+TN)$), and F1 score ($2 \times [\text{precision} \times \text{recall}] / [\text{precision} + \text{recall}]$) of the predictive model were derived. For comparison, we created a model that used only demographic data (e.g., age, sex) and conventional MRI features (e.g., callosal angle, Evans index, presence or absence of DESH). As a supplementary analysis, we also tested several alternative models with various permutations of the features.

Results

Demographic Characteristics

There were 87 responders and 45 nonresponders to temporary CSF drainage. There were no between-group differences in age, sex, baseline MoCA, Evans index, presence of DESH, baseline total CSF volume, baseline total GMV, or baseline white matter T2-weighted hyperintensity vol-

TABLE 1. Demographic and clinical data

Variable	Responder	Nonresponder	Test Statistic	p Value
No. of patients	87	45		
Age, yrs	77.5 (5.9)	77.6 (4.9)	t = -0.14	0.89
Male/female sex	53/34	29/16	$\chi^2 = 0.16$	0.84
ELD/LP procedure	82/5	34/11	$\chi^2 = 9.7$	0.002
MoCA score	18.7 (5.1)	19.8 (5.1)	t = -1.04	0.30
Change in MoCA score*	2.12 (3.8)	0.19 (2.1)	t = 2.65	0.009
Gait velocity, m/sec†	0.51 (0.38)	0.70 (0.45)	t = -2.4	0.018
Change in gait velocity, m/sec†	0.24 (0.27)	-0.03 (0.15)	t = 5.96	<0.001
rCSF, ml	0.32 (0.04)	0.33 (0.05)	t = -1.3	0.21
rWMH, cm ³	0.012 (0.009)	0.010 (0.008)	z = 0.31	0.76
Total rGMV, cm ³	0.38 (0.03)	0.37 (0.03)	t = 0.84	0.40
Callosal angle, °*	79.3 (22.1)	90.2 (24.8)	t = -2.6	0.012
Evans index	0.38 (0.04)	0.39 (0.05)	t = -1.56	0.12
Positive/negative DESH diagnosis	63/24	29/16	$\chi^2 = 0.89$	0.34

rCSF = relative CSF volume; rGMV = relative GMV; rWMH = relative white matter T2-weighted hyperintensity volume. Values are shown as number or mean (SD) unless indicated otherwise.

* Evaluated in the subset of 100 patients with preprocedural and postprocedural MoCA scores.

† Evaluated in the subset of 118 patients with procedural and postprocedural gait velocity data.

ume (Table 1). Nonresponders had higher baseline gait velocity ($p = 0.018$) and were more likely to have received LP than ELD ($p = 0.002$). In this cohort, negative LP patients underwent subsequent ELD that was also negative. Nonresponders had greater callosal angles ($p = 0.012$). Responders had greater increases in MoCA score ($p = 0.009$) and gait velocity ($p < 0.001$) than nonresponders (Table 1).

VBM Analysis of Responders Versus Nonresponders

One hundred thirty-two subjects were included in the VBM analysis of GMV differences between the responder and nonresponder groups. The nonresponders demonstrated decreased GMV in the right supplementary motor area (SMA) and right posterior parietal cortex as compared with responders ($p < 0.001$, $p < 0.05$ FDR cluster correction) (Fig. 1, Table 2). We did not observe significant group differences when the whole-brain analysis was repeated with random shuffling of the responder/nonresponder labels. When the LP patients were removed, the same clusters were seen but the cluster p value did not meet the FDR-corrected threshold (Supplementary Fig. 2).

Association of GMV With Clinical Change

To assess the relationship between baseline regional GMV and change in MoCA, we utilized 100 subjects who had preprocedural and postprocedural MoCA data. The change in MoCA was related to average baseline GMV in the posterior parietal cortex ($r^2 = 0.076$, $p = 0.005$) (Fig. 2A) but not in the SMA ($r^2 = 0.014$, $p = 0.25$). To assess the relationship between baseline regional GMV and change in gait velocity, we utilized 118 subjects who had preprocedural and postprocedural gait velocity data. The change in gait velocity was also related to the average baseline GMV in the posterior parietal cortex ($r^2 = 0.075$, $p = 0.0027$) (Fig. 2B) but not in the SMA ($r^2 = 0.0007$, $p = 0.34$).

Machine Learning Analysis

The SVM was built with the extracted average GMV from the right SMA and the right posterior parietal cortex, along with callosal angle and age. LOOCV was used for validation. The accuracy of the model was 75.8%, specificity was 42.2%, and recall/sensitivity was 93.1%. The precision/PPV of the model was 75.7%, NPV was 76.0%, and F1 score was 0.835. The overall error rate was 24.2% (Fig. 3A). The accuracy remained at 75% when all LP patients were excluded. By comparison, the model withholding GMV values and incorporating age, sex, callosal angle, DESH, and Evans index achieved an accuracy of response classification of 62.9%, error rate of 37.1%, specificity of 4.4%, sensitivity/recall of 93.1%, precision/PPV of 65.3%, NPV of 25.0%, and F1 score of 0.767 (Fig. 3B). The results of all alternative models are found in Supplementary Table 2. The top-performing model required the inclusion of GMV from both the SMA and posterior parietal cortex, as well as callosal angle measurement.

Data Availability

De-identified, postprocessed MRI scans and associated clinical information are available on reasonable request. Preprocessing and ComBat harmonization function scripts are available upon reasonable request.

Discussion

In this study, we utilized a large clinical database of suspected iNPH patients to assess the relationship between baseline GMV and response to temporary CSF drainage for the first time. We found that nonresponse was associated with decreased GMV in the right posterior parietal cortex and SMA. Furthermore, we found that baseline GMV of the right posterior parietal cortex was related to

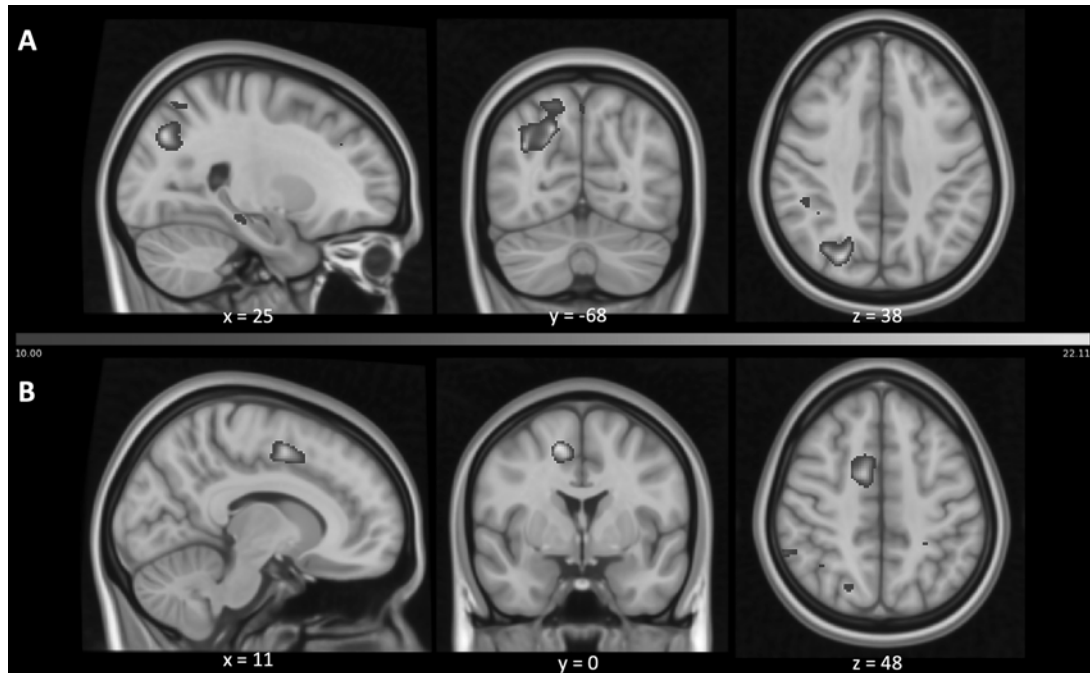


FIG. 1. Responder versus nonresponder. Nonresponders demonstrated decreased GMV in the right posterior parietal cortex (A) and right SMA (B). The color bar represents the F statistic and is overlaid onto the MNI template. The statistical threshold for significance was $p < 0.001$ and $p < 0.05$ with FDR correction (cluster). Figure is available in color online only.

changes in MoCA score and gait velocity after temporary CSF drainage. We subsequently used a machine learning model to predict response classification with an accuracy of 75.8% and F1 score of 0.835.

iNPH is one of the few forms of cognitive impairment with an effective treatment.²⁹ However, identification of patients who may respond to treatment remains a challenge. To avoid the potential morbidity associated with the unnecessary insertion of a permanent VPS, patients with suspected iNPH (based on radiographic evidence of enlarged ventricles in the context of appropriate symptomatology) should undergo testing with temporary CSF drainage. Identifying the features predictive of response to temporary drainage may help improve patient selection and clinical outcomes. Furthermore, by identifying factors that can influence clinical response, we may gain a better understanding of the pathophysiological mechanisms of the disease. Previously published studies in the literature have shown inconsistent predictors of response to CSF drainage.³⁰ Factors such as the Evans index, callosal angle, and presence or absence of DESH have been variously related to clinical outcome.³⁰ In this cohort, we found that demographic data, baseline total CSF volume, periventricular T2-weighted hyperintensities, total GMV,

Evans index, and presence or absence of DESH were not related to clinical response, whereas steeper callosal angle was. We predicted clinical outcomes using basic demographic and conventional MRI data and found poor classification accuracy and a moderate F1 score. When regional GMV values were included in the predictive model, classification performance increased substantially. Specifically, patients who were classified as having FP results by the comparison model were more accurately identified as having TN results, thereby increasing specificity and NPV. This suggests that reduced GMV is particularly valuable for identifying patients who will not respond to temporary CSF drainage. In our supplementary analysis, we identified that the top model requires GMV from both the SMA and the posterior parietal cortex, along with the callosal angle. The importance of a steep callosal angle is increasingly recognized in the evaluation of iNPH.^{31,32} Our findings support the utility of the callosal angle and further suggest that consideration of baseline regional GMV can improve the prediction of clinical outcomes and can help with patient selection.

Along with the clinical utility of this finding, it may also provide some new insights into the neural substrate contributing to iNPH symptoms. The posterior parietal

TABLE 2. Responder versus nonresponder

Region	MNI Coordinates (x, y, z)	Voxel p Value (uncorrected)	Cluster Extent	Cluster p Value (FDR corrected)
Rt SMA	15, 0, 52	0.000007	514	0.0497
Rt posterior parietal cortex	20, -69, 40	0.00001	829	0.014

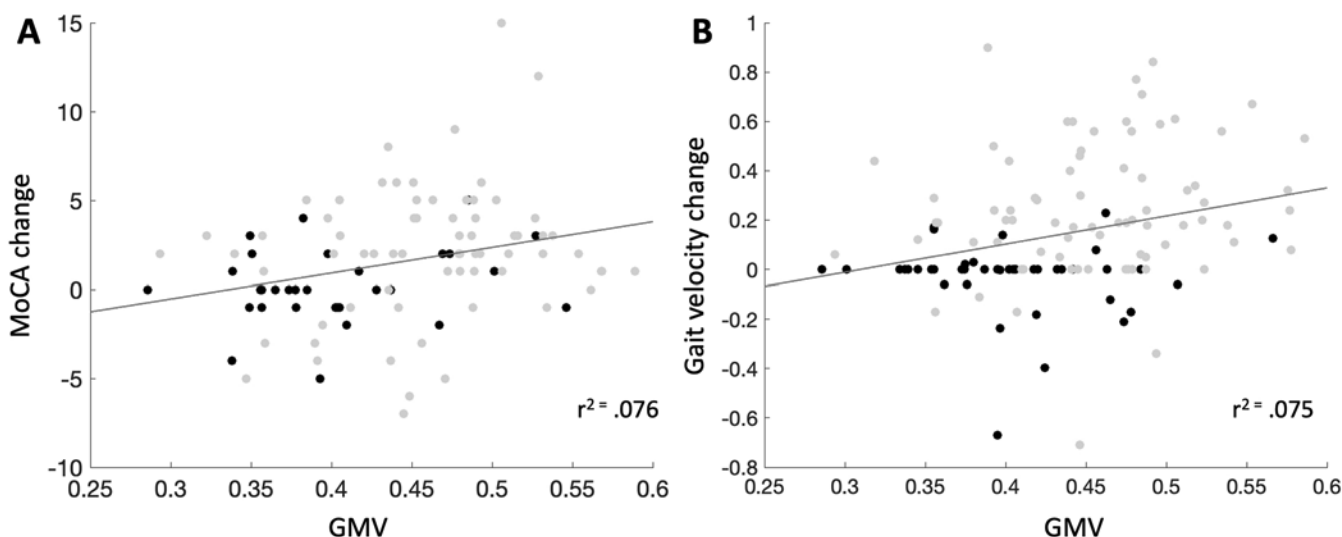


FIG. 2. Relationship of cortical volume with clinical change. **A:** GMV in the posterior parietal cortex was related to change in MoCA. **B:** GMV in the posterior parietal cortex was related to change in gait velocity. *Yellow marks indicate responders; black marks indicate nonresponders.* Figure is available in color online only.

cortex is a major associative region of the human brain implicated in integrating cognitive, somatosensory, visual, proprioceptive, and vestibular signals,³³ and it has been shown to be particularly important for gait function. Specific parameters of gait in iNPH have been associated with the thickness of the posterior parietal cortex.³⁴ Furthermore, activity in the right posterior parietal cortex is related to severity of gait disturbance in Parkinson's disease,³⁵ while volume reduction of this region contributes to freezing of gait.³⁶ These findings suggest that dysfunction of the posterior parietal cortex is a shared pathophysiological substrate of gait dysfunction between iNPH and Parkinson's disease. A difference in the GMV of the SMA between responders and nonresponders was also found, although this difference was not related to change in

MoCA score or gait velocity. Classification of CSF drainage response was not made solely on the basis of absolute changes in MoCA score and gait velocity, so it is possible that reduced GMV in this region may limit improvement in domains not quantitatively measured here. The SMA has been implicated in a variety of motor functions,^{37–39} suggesting that reduced GMV in this region could contribute to reduced motor function improvement not quantified specifically by gait velocity. Consistent with this, a study utilizing functional MRI before and after ELD in iNPH patients demonstrated that increased activation of the SMA was associated with motor function recovery defined by upper-extremity reaction times.⁴⁰ In the context of this work, our results suggest that decreased volume of the SMA restricts the capacity to increase activity

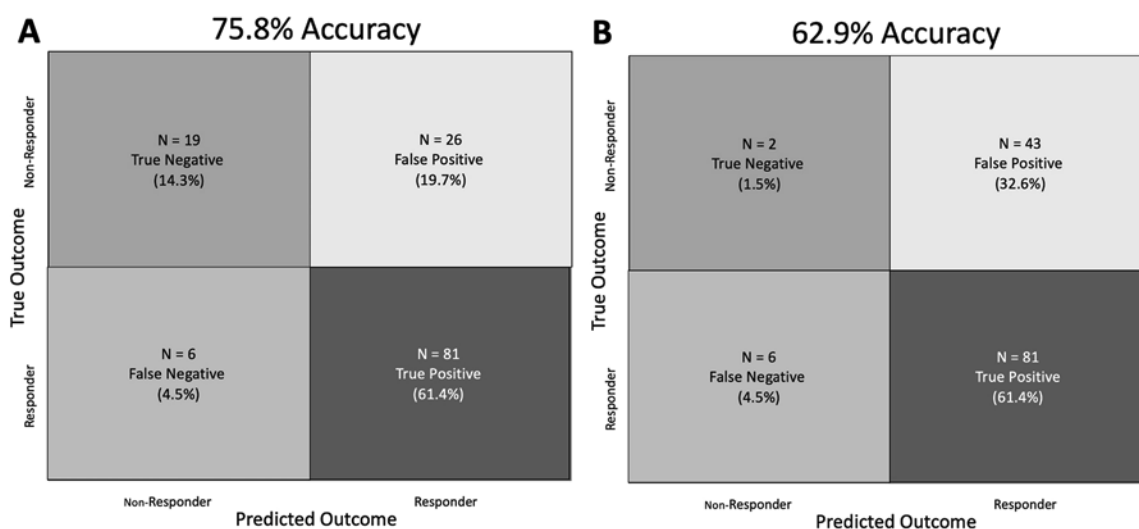


FIG. 3. Prediction of response using machine learning. **A:** Extracted GMV from the right posterior parietal cortex and SMA, along with age and callosal angle, was fed into an SVM model and validated with LOOCV. **B:** The comparison model used demographic data and conventional MRI measurements. Figure is available in color online only.

and thereby limits clinical improvement. Speculatively, it is possible that dysfunction of the SMA and posterior parietal cortex contributes to the phenotype of iNPH and clinical treatments are no longer effective when this dysfunction reaches a critical limit, as manifested through decreased GMV. It is possible that this reduced GMV may be the end result of the myriad pathophysiological events underlying iNPH.² This hypothesis will need to be assessed with longitudinal imaging studies but, if true, may help in early identification and patient selection for treatment. Importantly, there was no difference in total GMV between responders and nonresponders, suggesting that specific regional reductions are crucial rather than a general pattern of gray matter atrophy.

This study had several limitations. Nonresponders were more likely to receive a large-volume lumbar tap than ELD. We adjusted for this difference statistically, and we found a similar trend of reduced GMV when we removed this group. Furthermore, these patients were subsequently classified as nonresponders on the basis of an ELD trial. We also found that baseline gait velocity was higher in the nonresponder group compared with the responder group. This is consistent with a multicenter registry study, which found lower baseline gait velocity in patients selected for shunt surgery than those who were not selected.¹⁶ The reason for this difference is unclear, but several possibilities emerge. First, the nonresponder group may have demonstrated the ceiling effect, whereby their gait cannot improve from the higher baseline. It is also possible that the subjects for which gait information was unavailable were more likely to be nonresponders, potentially biasing the data. While the decision to classify a patient as a responder or nonresponder was based primarily on quantitative criteria, the clinical expertise of the senior author also played a role in patient classification. This reflects the reality of clinical practice, where decisions are made in the absence of a complete set of data.¹⁶

This study reports outcomes after temporary CSF drainage. All responders were subsequently offered a VPS. Although the shunt outcomes are not reported here, they were previously summarized as part of a larger cohort study of VPS at our institution.⁴¹ Future work is necessary to determine whether GMV also helps to predict nonresponse to permanent CSF diversion, although this will require a larger sample size due to the lower rate of nonresponse. Next, this was a retrospective single-center study that took advantage of a large clinical database of suspected iNPH patients. Due to the retrospective nature of the study, we did not have a predefined MRI acquisition strategy and we used data from several different clinical scanners. Although this is normally considered a limitation in computational MRI analysis due to the introduction of nonbiological variability, novel harmonization procedures have been shown to overcome this. We believe this was a strength of the investigation. By utilizing the ComBat harmonization algorithm, we showed that it is possible to use data collected for clinical purposes from multiple scanners in a research capacity. Harmonization algorithms thus give investigators the ability to explore existing data that may have been overlooked otherwise. Finally, these findings will need to be confirmed on a prospective cohort and,

while the predictive model was validated with LOOCV, it will need to be assessed on an independent data set.

Conclusions

Decreased GMV in the SMA and posterior parietal cortex may help identify patients with suspected iNPH likely to experience a negative response after temporary CSF drainage. These patients may have limited capacity for recovery due to atrophy or preexisting decreased GMV in these regions known to be important for motor and cognitive integration. Although prospective validation is necessary, this study represents an important step toward improving patient selection and predicting clinical outcomes in the treatment of iNPH.

References

- Gallia GL, Rigamonti D, Williams MA. The diagnosis and treatment of idiopathic normal pressure hydrocephalus. *Nat Clin Pract Neurol*. 2006;2(7):375-381.
- Wang Z, Zhang Y, Hu F, Ding J, Wang X. Pathogenesis and pathophysiology of idiopathic normal pressure hydrocephalus. *CNS Neurosci Ther*. 2020;26(12):1230-1240.
- Isaacs AM, Riva-Cambrin J, Yavin D, et al. Age-specific global epidemiology of hydrocephalus: systematic review, meta-analysis and global birth surveillance. *PLoS One*. 2018;13(10):e0204926.
- Jacobsson J, Qvarlander S, Eklund A, Malm J. Comparison of the CSF dynamics between patients with idiopathic normal pressure hydrocephalus and healthy volunteers. *J Neurosurg*. 2019;131(4):1018-1023.
- Qvarlander S, Lundkvist B, Koskinen L-OD, Malm J, Eklund A. Pulsatility in CSF dynamics: pathophysiology of idiopathic normal pressure hydrocephalus. *J Neurol Neurosurg Psychiatry*. 2013;84(7):735741.
- Owler BK, Momjian S, Czosnyka Z, et al. Normal pressure hydrocephalus and cerebral blood flow: a PET study of baseline values. *J Cereb Blood Flow Metab*. 2004;24(1):17-23.
- Owler BK, Pickard JD. Normal pressure hydrocephalus and cerebral blood flow: a review. *Acta Neurol Scand*. 2001;104(6):325-342.
- Ringstad G, Vatnehol SAS, Eide PK. Glymphatic MRI in idiopathic normal pressure hydrocephalus. *Brain*. 2017;140(10):2691-2705.
- Eide PK, Ringstad G. Delayed clearance of cerebrospinal fluid tracer from entorhinal cortex in idiopathic normal pressure hydrocephalus: a glymphatic magnetic resonance imaging study. *J Cereb Blood Flow Metab*. 2019;39(7):1355-1368.
- Siasios I, Kapsalaki EZ, Fountas KN, et al. The role of diffusion tensor imaging and fractional anisotropy in the evaluation of patients with idiopathic normal pressure hydrocephalus: a literature review. *Neurosurg Focus*. 2016;41(3):E12.
- Kanno S, Abe N, Saito M, et al. White matter involvement in idiopathic normal pressure hydrocephalus: a voxel-based diffusion tensor imaging study. *J Neurol*. 2011;258(11):1949-1957.
- Ishii K, Kawaguchi T, Shimada K, et al. Voxel-based analysis of gray matter and CSF space in idiopathic normal pressure hydrocephalus. *Dement Geriatr Cogn Disord*. 2008;25(4):329-335.
- Khoo HM, Kishima H, Tani N, et al. Default mode network connectivity in patients with idiopathic normal pressure hydrocephalus. *J Neurosurg*. 2016;124(2):350-358.
- Griffa A, Van De Ville D, Herrmann FR, Allali G. Neural circuits of idiopathic normal pressure hydrocephalus: a perspective review of brain connectivity and symptoms meta-analysis. *Neurosci Biobehav Rev*. 2020;112:452-471.

15. Williams MA, Malm J. Diagnosis and treatment of idiopathic normal pressure hydrocephalus. *Continuum (Minneapolis)*. 2016;22(2 Dementia):579-599.
16. Williams MA, Nagel SJ, Golomb J, et al. Safety and effectiveness of the assessment and treatment of idiopathic normal pressure hydrocephalus in the Adult Hydrocephalus Clinical Research Network. *J Neurosurg*. 2022;137(5):1289-1301.
17. Isaacs AM, Williams MA, Hamilton MG. Current update on treatment strategies for idiopathic normal pressure hydrocephalus. *Curr Treat Options Neurol*. 2019;21(12):65.
18. Fortin JP, Cullen N, Sheline YI, et al. Harmonization of cortical thickness measurements across scanners and sites. *Neuroimage*. 2018;167:104-120.
19. Johnson WE, Li C, Rabinovic A. Adjusting batch effects in microarray expression data using empirical Bayes methods. *Biostatistics*. 2007;8(1):118-127.
20. Fortin JP, Parker D, Tuñç B, et al. Harmonization of multi-site diffusion tensor imaging data. *Neuroimage*. 2017;161:149-170.
21. Yu M, Linn KA, Cook PA, et al. Statistical harmonization corrects site effects in functional connectivity measurements from multi-site fMRI data. *Hum Brain Mapp*. 2018;39(11):4213-4227.
22. Bell TK, Godfrey KJ, Ware AL, Yeates KO, Harris AD. Harmonization of multi-site MRS data with ComBat. *Neuroimage*. 2022;257:119330.
23. Radua J, Vieta E, Shinohara R, et al. Increased power by harmonizing structural MRI site differences with the ComBat batch adjustment method in ENIGMA. *Neuroimage*. 2020;218:116956.
24. Ashburner J, Friston KJ. Voxel-based morphometry—the methods. *Neuroimage*. 2000;11(6 Pt 1):805-821.
25. Gaser C, Dahnke R, Thompson PM, Kurth F, Luders E. CAT—A Computational Anatomy Toolbox for the analysis of structural MRI data. *bioRxiv*. Preprint posted online June 13, 2022. doi:10.1101/2022.06.11.495736
26. Dahnke R, Ziegler G, Grosskreutz J, Gaser C. Retrospective quality assurance of MR images. Poster presented at: 19th Annual Meeting of the Organization for Human Brain Mapping; June 16–20, 2013; Seattle, WA.
27. Ashburner J. A fast diffeomorphic image registration algorithm. *Neuroimage*. 2007;38(1):95-113.
28. Dahnke R, Ziegler G, Gaser C. Detection of white matter hyperintensities in T1 without FLAIR. Paper presented at: 2019 Organization for Human Brain Mapping Annual Meeting; June 9–13, 2019; Rome, Italy.
29. Shprecher D, Schwab J, Kurlan R. Normal pressure hydrocephalus: diagnosis and treatment. *Curr Neurol Neurosci Rep*. 2008;8(5):371-376.
30. Oertel JMK, Huelser MJM. Predicting the outcome of normal pressure hydrocephalus therapy—where do we stand? *Acta Neurochir (Wien)*. 2021;163(3):767-769.
31. Virhammar J, Laurell K, Cesarini KG, Larsson EM. The callosal angle measured on MRI as a predictor of outcome in idiopathic normal-pressure hydrocephalus. *J Neurosurg*. 2014;120(1):178-184.
32. Hattori T, Ohara M, Yuasa T, et al. Correlation of callosal angle at the splenium with gait and cognition in normal pressure hydrocephalus. *J Neurosurg*. Published online January 20, 2023. doi:10.3171/2022.12.JNS221825
33. Whitlock JR. Posterior parietal cortex. *Curr Biol*. 2017;27(14):R691-R695.
34. Yun EK, Kang K, Yoon U. Correlation analysis between gait pattern and structural features of cerebral cortex in patients with idiopathic normal pressure hydrocephalus. *J Biomed Eng Res*. 2021;42(6):295-303.
35. Crémers J, D’Ostilio K, Stamatakis J, Delvaux V, Garraux G. Brain activation pattern related to gait disturbances in Parkinson’s disease. *Mov Disord*. 2012;27(12):1498-1505.
36. Rubino A, Assogna F, Piras F, et al. Does a volume reduction of the parietal lobe contribute to freezing of gait in Parkinson’s disease? *Parkinsonism Relat Disord*. 2014;20(10):1101-1103.
37. Nachev P, Wydell H, O’neill K, Husain M, Kennard C. The role of the pre-supplementary motor area in the control of action. *Neuroimage*. 2007;36(suppl 2)(3-3):T155-T163.
38. Nachev P, Kennard C, Husain M. Functional role of the supplementary and pre-supplementary motor areas. *Nat Rev Neurosci*. 2008;9(11):856-869.
39. Goldberg G. Supplementary motor area structure and function: review and hypotheses. *Behav Brain Sci*. 1985;8(4):567-588.
40. Lenfeldt N, Larsson A, Nyberg L, et al. Idiopathic normal pressure hydrocephalus: increased supplementary motor activity accounts for improvement after CSF drainage. *Brain*. 2008;131(Pt 11):2904-2912.
41. Hamilton MG, Lang ST, Ben-Israel D, et al. Outcomes associated with a standardized assessment and treatment protocol for 298 patients with suspected idiopathic normal pressure hydrocephalus (iNPH): Abstracts from The Thirteenth Meeting of the International Society for Hydrocephalus and Cerebrospinal Fluid Disorders. *Fluids Barriers CNS*. 2021;18(suppl 2):O42.

Disclosures

Dr. Kalia reported personal fees from Medtronic, Abbott, and Novo Nordisk; nonfinancial support from Boston; and grants from Parkinson Canada, CIHR, MJFF, and CFI outside the submitted work. Dr. Lozano reported personal consultant fees from Abbott, Boston Scientific, Insightec, Medtronic, and Functional Neuromodulation as scientific director outside the submitted work. Dr. Hamilton reported personal fees from Integra Canada for an INPH workshop and Medtronic International for an INPH webinar, grants from Alberta Innovates for reducing infections in shunts and CSF drains, and work on the data and safety monitoring board of CereVasc outside the submitted work.

Author Contributions

Conception and design: Hamilton, Lang. Acquisition of data: Hamilton, Isaacs, Dronyk. Analysis and interpretation of data: Lang, Dimond, Isaacs, Fasano, Kalia, Lozano. Drafting the article: Hamilton, Lang, Conner. Critically revising the article: Hamilton, Lang, Dimond, Isaacs, Vetkas, Conner, Germann, Fasano, Kalia, Lozano. Reviewed submitted version of manuscript: Hamilton, Lang, Dimond, Isaacs, Vetkas, Germann, Fasano, Kalia, Lozano. Approved the final version of the manuscript on behalf of all authors: Hamilton. Statistical analysis: Lang. Administrative/technical/material support: Hamilton, Dronyk. Study supervision: Hamilton, Kalia, Lozano.

Supplemental Information

Online-Only Content

Supplemental material is available with the online version of the article.

Supplementary Tables and Figures. <https://thejns.org/doi/suppl/10.3171/2023.3.JNS222787>.

Previous Presentations

An early version of this paper was presented as an abstract at the 2022 Congress of Neurological Surgeons Annual Meeting, San Francisco, CA, October 8–12, 2022.

Correspondence

Mark G. Hamilton: University of Calgary, AB, Canada. mghamilton.hydro@gmail.com.